WP/20/159

IMF Working Paper

The Effect of Containment Measures on the COVID-19 Pandemic

by Pragyan Deb, Davide Furceri, Jonathan D. Ostry, Nour Tawk

INTERNATIONAL MONETARY FUND

 WP/20/159

IMF Working Paper

Asia and Pacific Department

The Effect of Containment Measures on the COVID-19 Pandemic*

Prepared by **Pragyan Deb, Davide Furceri, Jonathan D. Ostry, Nour Tawk**

Authorized for distribution by Jonathan D. Ostry

August 2020

Abstract

Countries have implemented several containment measures to halt the spread of the 2019 coronavirus disease, but it remains unclear the extent to which these unprecedented measures have been successful. We examine this question using daily data on the number of coronavirus disease cases as well as on real-time containment measures implemented by countries. Results suggest that these measures have been very effective in flattening the "pandemic curve", but there is significant heterogeneity across countries. Effectiveness is enhanced when measures are implemented quickly, where de facto mobility is curtailed, in countries with lower temperatures and population density, as well as in countries with a larger share of the elderly in total population and stronger health systems. We also find that easing of containment measures has resulted in an increase in the number of cases, but the effect has been lower (in absolute value) than that from a tightening of measures.

JEL Classification Numbers: E52, E58, D43, L11
Keywords: Covid-19; pandemics; containment measures
Author's E-Mail Address:pdeb@imf.org; dfurceri@imf.org; jostry@imf.org; ntawk@imf.org

* We are grateful to Naihan Yang for excellent research assistance. We would like to thank anonymous referees for COVID economics, Francesca Caselli, Chiara Fratto, Francesco Grigoli, and, Mico Mrkaic, Chris Redl, Damiano Sandri, Yunhui Zhao, and seminar participants at the IMF for helpful comments and suggestions. An earlier version of this paper was published in Covid Economics and is available here: https://cepr.org/sites/default/files/news/CovidEconomics19.pdf#Paper2

Table of Contents

I. INTRODUCTION

Since the outbreak was first reported in Wuhan, China in late-December 2019, the corona virus disease (COVID-19) has spread to over 200 countries and territories globally (Figure 1, panel A). As of June 26, close to 10 million cases have been confirmed, resulting in nearly 500 thousand deaths.

In the absence of a vaccine or effective treatments, many countries have responded by implementing several non-pharmaceutical interventions to halt the spread of the virus and limit the number of fatalities. Interventions included improved diagnostic testing and contact tracing, isolation and quarantine for infected people, and most notably measures aimed at reducing mobility and creating social distancing (containment measures, hereafter). While the extent and type of containment measures introduced varies across countries, most countries have introduced a combination of: (i) school closures; (ii) workplace closures; (iii) cancellation of public events; (iv) restrictions on size of gatherings ; (v) closures of public transport; (vi) stay-at-home orders; (vii) restrictions on internal movement; (viii) restrictions on international travel. Figure 1 (panel B) presents the broad patterns of containment measures across time and country groups, based on a composite index of these measures (see next section for detail).

To date, there is limited evidence on the quantitative effect of these measures, and it remains unclear why they seem to have been more successful in certain countries compared with others. Indeed, despite significant theoretical contributions on the topic, to the best of our knowledge, empirical evidence on the quantitative effect of these measures is limited to China and a few economies (see next section for a brief review). It is also unclear why containment measures seem to have been more successful in certain countries compared to others. Indeed, while almost all countries have adopted stringent containment measures, there is huge variation on the observed

evolution of the pandemic, suggesting that country-specific factors may have played an important role in explaining the effectiveness of these measures.

We try to address this knowledge gap by using daily data on the number of COVID-19 cases and deaths as well as on real-time containment measures in 129 countries around the world from January 1 to June 15, 2020. The large sample of countries allows us to analyze some key factors contributing to the heterogeneity in the effectiveness of containment measures. We also use these data to assess the role of re-openings (easing of containment measures) in the resurgence of infections in many economies.

Establishing causality is difficult in this context because, as illustrated in Figure 1, countries have introduced containment measures in response to the spread of the virus. This implies that addressing causality requires the researcher to effectively control for this endogenous response. Failure to control for possible reverse causality would result in estimates of the effect of containment measures on infections and deaths being upward biased—that is, toward *not* finding significant effectiveness. We address this issue by controlling for the change in the number of infected cases occurring in the days before the implementation of containment measures. Given lags in the implementation of interventions at daily frequency, this allows one to effectively control for the endogenous response of containment measures to the spread of the virus. To further account for expectations about the country-specific evolution of the pandemic, we also control for country-specific linear, quadratic, and cubic time trends.

Another important empirical challenge is that containment measures have been introduced as parts of broader non-pharmaceutical interventions (NPIs) including enhanced testing, contact tracing and public information campaign aimed at increasing social awareness. To address this issue and disentangle the effect of containment measures from other NPIs, we explicitly control for these variables in our estimation framework.

Finally, there are concerns that containment measures were announced before being implemented and were, therefore, anticipated. This may have resulted in reduced mobility ahead of the implementation of some containment measures and to an upward bias in the estimates. We show that controlling for mobility does not quantitatively change the results. Further, an analysis on the effect international travel restrictions, which were implemented across countries in response to outbreaks in other countries—and therefore exogenous to domestic conditions—and ahead of the other containment measures and reduced mobility, provides reassurance on the causal effect of containment measures.

Results suggest that containment measures have been, on average, very effective in flattening the "pandemic curve". These effects have been stronger in countries where containment measures have been implemented faster and have resulted in less *de facto* mobility—more social distancing—and in countries with lower temperatures, lower population density, a larger share of the elderly in the population, and stronger health systems. Across different types of containment measure, internal and international travel restrictions have been most effective. We also show that easing of containment measures (re-openings) has resulted in an increase in the number of cases, but the effect has been lower (in absolute value) than that from tightening measures.

The remainder of the paper is structured as follows. Section II provides a brief review of the rapidly growing literature on the effect on containment measures on the COVID-19 pandemic. Section III describes the data and econometric methodology. Section IV presents our results on the effect of containment measures on COVID-19 cases, and how these effects vary across countries (depending on country-specific characteristics) and type of containment measure. It also extends the analysis to assess the impact on the number of fatalities. The last section concludes.

II. RELATED LITERATURE

The literature on the effectiveness of containment measures is rapidly expanding. The empirical strand of these studies focuses on the impact of measures in China. Kraemer *et al.* (2020) match real-time mobility data from Wuhan with detailed case data of travel history to showcase the role of mobility in the transmission of COVID-19 across cities in China, as well as the impact of control measures on the spread of the epidemic. They find that while mobility played a large role in the spread of the virus initially, after the implementation of control measures, the correlation between infection growth rates and mobility dropped significantly.

Chinazzi *et al.* (2020) use a global metapopulation disease model to project the impact of travel restrictions on the spread of COVID-19. The model estimates that while travel restrictions reduced case importations outside China significantly, they would not impact the trajectory of the pandemic if they are not combined with a reduction in the transmissibility of the disease.

Tian et al. (2020) investigate the role of the Wuhan travel ban and public health non-pharmaceutical interventions (NPI) in China on the reproduction number (R_0) of COVID-19, using a geocoded repository of COVID-19 data. They find that the reproduction number fell significantly after travel restrictions and public health interventions were implemented.

Cowling et al. (2020) use cross-sectional telephone surveys to model social behavior towards COVID-19 in Hong Kong SAR, and then examine the impact of NPIs and social behavior on COVID-19 transmission. They find that social distancing measures and behavioral changes coincided with a substantial drop in influenza transmission in February 2020, which suggests a similar impact on COVID-19 transmission rates.

More closely to our work, Hsiang et al. (2020) compile new data on 1,717 local, regional, and national non-pharmaceutical interventions deployed in China, Korea, Italy, Iran, France and

the United States, to estimate the effect of containment measures on the growth rate of infection. They estimate that, in the absence of policy actions, early infections of COVID-19 exhibit exponential growth of roughly 38 percent per day, and find that anti-contagion policies have significantly reduced this growth.

There have been also numerous studies using modelling approaches to examine the impact of containment measures. Here we provide a selected survey of recent papers, and we refer to them for a more extensive review. Eichenbaum, Rebelo and Trabandt (2020) extend the classic SIR model by Kermack and McKendrick (1927) to study the equilibrium interactions between economic decisions and the dynamics of epidemics. Their model finds that, while people's decisions to cut back on work and consumption reduce fatalities, they exacerbate the recession during an epidemic.

Forslid and Herzing (2020) use a basic epidemiologic model calibrated to resemble COVID-19 dynamics to study the implications of quarantines. They find that the implementation of early quarantine can delay but not alter the course of a pandemic, while delaying quarantine reduces both deaths and economic costs but results in a higher peak infection.

Brotherhood et al. (2020) calibrate a standard SIR epidemiological model to investigate the role of testing and quarantine measures. They find that imposing restrictions for the young (given limited mobility of the elderly) can prolong the epidemic as herd immunity is delayed and expose the elderly to extended periods of risk. They also find that testing and quarantine would significantly reduce infections, even if only targeted to the young, who are highly mobile. Finally, their results suggest that quarantines are most efficient close to when a vaccine is in place, so that the disease has a lower chance of rebounding.

III. DATA AND METHODOLOGY

A. Data

We assemble a comprehensive daily database across many areas.

COVID-19 infections and deaths

Data on infections and deaths are collected from the COVID-19 Dashboard[1], which is sourced by the Coronavirus Resource Center of Johns Hopkins University. Coverage begins from January 22, 2020 and provides the location and number of confirmed cases, deaths, and recoveries for 208 affected countries and regions. For this paper, the data cut-off is June 16, 2020.

Containment measures

We use data Oxford's COVID-19 Government Response Tracker[2] (OxCGRT) for containment measures. OxCGRT collects information on government policy responses across eight dimensions, namely: (i) school closures; (ii) workplace closures; (iii) public event cancellations; (iv) gathering restrictions; (v) public transportation closures; (vi) stay-at-home orders; (vii) restrictions on internal movement; and (viii) international travel bans. The database scores the stringency of each measure ordinally, for example, depending on whether the measure is a recommendation or a requirement and whether it is targeted or nationwide. We normalize each measure to range between 0 and 1 to make them comparable. In addition, we use the

[1] COVID-19 Map, JHU Coronavirus Resource Center, Accessed June 16, 2020 https://coronavirus.jhu.edu/map.html.
[2] "Coronavirus Government Response Tracker." Blavatnik School of Government. Accessed June 16, 2020. https://www.bsg.ox.ac.uk/research/research-projects/coronavirus-government-response-tracker.

aggregate Stringency Index calculated as the average of the sub-indices, again normalized to range between 0 and 1. This database starts on January 1, 2020 and covers 151 economies.

Additional controls used are:

Additional non-pharmaceutical interventions

We include daily data for the following non-pharmaceutical interventions: testing policies, contacting tracing policies, and public information campaigns. The data are collected from OxCGRT and are available for 176 countries from January 1, 2020.

Temperature and humidity

We include daily data on mean temperature and humidity for 95 countries. The data are collected from the Air Quality Open Data Platform and include humidity and temperature for each major city, based on the median of several stations, in 95 countries from January 1, 2020.[3]

Tests conducted

We use daily data on COVID-19 tests from Our World in Data, an open source platform drawn from countries' Ministry of Health.[4] The dataset covers total tests conducted and tests per thousand people in 84 countries from January 1, 2020 onwards. Given limited data coverage on testing, this variable is not used in the baseline specification and but in the robustness check analysis.

[3] *COVID-19 Worldwide Air Quality Data*. Accessed June 16, 2020. https://aqicn.org/data-platform/COVID-19/report/

[4] Hasell, Joe, COVID-19 Testing - Statistics and Research." https://ourworldindata.org/coronavirus-testing.

Population density and age structure

We use indicators which are relevant to the COVID-19 pandemic, such as population density and age structure. Indicators are sourced from The World Development Indicators database,[5] which is developed by the World Bank Group and compiled from official international sources. Data coverage includes 189 member countries, with the latest available data.

Health robustness indices

We use two different indices for health robustness. The first is the Global Health Security index, published by the Johns Hopkins Center for Health Security, which provides a comprehensive assessment of health security across 195 countries.[6] It generates an index based on countries' health scores for the following six categories: (i) prevention of the emergence or release of pathogens; (ii) early detection and reporting for epidemics of potential international concern; (iii) rapid response to and mitigation of the spread of an epidemic; (iv) sufficient and robust health system to treat the sick and protect health workers; (v) commitments to improving national capacity, financing plans to address gaps, and adhering to global norms; and (vi) overall risk environment and country vulnerability to biological threats.

We also use the Health Index, which measures the overall health condition of economies on a 0-7 scale. It is sourced from the 2019 Global Competitiveness Report by the World Economic Forum and covers 114 economies.[7]

[5] "World Development Indicators." Washington, D.C.: The World Bank. Accessed June 16, 2020.
[6] "The Global Health Security Index." GHS Index. Accessed June 16, 2020. https://www.ghsindex.org.
[7] Schwab, Klaus; Sala i Martin, Xavier; World Economic Forum, "Global Competitiveness Report 2019", World Economic Forum, 10/2019. Accessed June 16, 2020.

Mobility Trends

We use data provided by Apple Map's Mobility Trends Report and Google Mobility Reports.[8] Apple's daily report produces walking and driving indices for 66 countries, sent from user's devices to the Apple map server. Specifically, it measures the relative volume of direction requests. Data are available both for walking as well as driving directions. The report started from January 13, 2020.

This is supplemented by similar data from Google's mobility indices, specifically retail and transit-station mobility. These data series show how visits and lengths of stay have changed since containment measures have begun. Daily data is available for 89 countries in our dataset, with coverage beginning from February 15, 2020.

B. Methodology

Similar to Hsiang et al. (2020), we use a reduced-form econometric approach to identify the causal effect of containment measures on the evolution of the number of COVID-19 infections. In particular, we use a "difference-in-difference" approach that allows to compare the dynamic evolution of infected cases before and after the day of the introduction of the containment measure (treatment) in a given country (treatment group) with that of another country (control group) that has not instructed the measure in the same day. The approach can be thought as an experimental research design using observational study data.

Any analysis of the effect of containment measures on COVID-19 infections is clearly subject to reverse causality as countries (or states, regions and provinces) have introduced containment measures in

[8] Apple Maps Mobility Trends Report, Accessed June 16, 2020. https://www.apple.com/covid19/mobility.

response to the spread of the virus. This implies that addressing causality requires the researcher to effectively control for this endogenous response. Failure to control for possible reverse causality would result in estimates of the effect of containment measures on infections and deaths being upward biased—that is, toward *not* finding significant effectiveness. We address this issue by controlling for the change in the number of infected cases occurring in the day before the implementation of containment measures. Given lags in the implementation of interventions at a daily frequency, this allows one to effectively control for the endogenous response of containment measures to the spread of the virus. To further account for expectations about the country-specific (exponential) evolution of the pandemic, we also control for country specific linear, quadratic and cubic time trends.

An important empirical challenge is omitted variable bias, as containment measures have been introduced as parts of broader non-pharmaceutical interventions (NPIs) which include enhanced testing, contact tracing, and public information campaigns aimed towards increasing social awareness. To address this issue and disentangle the effect of containment measures from other NPIs, we explicitly control for these variables in our estimation framework.

Another concern is that containment measures were announced before being implemented and, therefore, were anticipated. This may have resulted in reduced mobility ahead of the implementation of some containment measures and to an upward bias in the estimates. We show that controlling for mobility does not quantitatively change the results. Moreover, examine the effect of international travel restrictions—which were implemented across countries in response to outbreaks in other countries, and therefore exogenous to domestic conditions, and ahead of the other containment measures and reduced mobility—and the results confirm that containment measures have been very effective in flattening the "pandemic curve" and reducing the number of fatalities.

Two econometric specifications are used to estimate the effect of containment measures on the number of confirmed COVID-19 cases and deaths. The first establishes whether containment had, on average, significant effects on infections. The second assesses whether these effects vary across countries depending on country-specific characteristics, such as the capacity of the health system, average temperature, the share of vulnerable (or elderly) persons in the population, etc. The analysis is also extended to the number of COVID-19 related fatalities.

We follow the approach proposed by Jordà (2005) to estimate the dynamic cumulative effect of containment measures on the number of confirmed COVID-19 cases, a methodology used also by Auerbach and Gorodnichenko (2013), Ramey and Zubairy (2018), and Alesina et al. (2019) among others. This procedure does not impose the dynamic restrictions embedded in vector autoregressions and is particularly suited to estimating nonlinearities in the dynamic response. The first regression we estimate is:

$$\Delta d_{i,t+h} = u_i + \theta_h c_{i,t} + X'_{i,t}\Gamma_h + \sum_{\ell=1}^{\mathcal{L}} \psi_{h,\ell}\Delta d_{i,t-\ell} + \varepsilon_{i,t+h} \qquad (1)$$

where $\Delta d_{i,t+h} = d_{i,t+h} - d_{i,t+h-1}$ and $d_{i,t}$ is the logarithm of the number of infections, in country i observed at date t. $c_{i,t}$ denotes the OxCGRT Stringency Index. u_i are country-fixed effects to account for time-invariant country-specific characteristics (for example, population density, age profile of the population, health capacity, average temperature, etc.). X is a vector of control variables which includes: (i) daily temperature and humidity levels; (ii) country-specific linear, quadratic and cubic time trends; (iii) testing and contact tracing policies and public information campaign.

The second specification allows for the response of COVID-19 infections to vary with countries characteristics. It is estimated as follows:

$$\Delta d_{i,t+h} = u_i + \theta_h^L F(z_{i,t}) c_{i,t} + \theta_h^H (1 - F(z_{i,t})) c_{i,t} + X'_{i,t}\Gamma_h + \sum_{\ell=1}^{\mathcal{L}} F(z_{i,t})\, \psi_{h,\ell} \Delta d_{i,t-\ell} + \sum_{\ell=1}^{\mathcal{L}} (1 - F(z_{i,t}))\psi_{h,\ell} \Delta d_{i,t-\ell} + \varepsilon_{i,t+h}$$

$$\text{with } F(z_{it}) = exp^{-\gamma z_{it}}/(1 - exp^{-\gamma z_{it}}), \quad \gamma > 0 \qquad (2)$$

where z is a country-specific characteristic normalized to have zero mean and a unit variance.

The weights assigned to each regime vary between 0 and 1 according to the weighting function $F(.)$, so that $F(z_{it})$ can be interpreted as the probability of being in a given state of the economy. The coefficients θ_h^L and θ_h^H capture the impact of containment measures at each horizon h in cases of very low levels of z ($F(z_{it}) \approx 1$ when z goes to minus infinity) and very high levels of z ($1 - F(z_{it}) \approx 1$ when z goes to plus infinity), respectively. $F(z_{it})$=0.5 is the cutoff between low and high country-specific characteristics—that is, for example, low and high health capacity.

This approach is equivalent to the smooth transition autoregressive model developed by Granger and Terävistra (1993). The advantage of this approach is twofold. First, compared with a model in which each dependent variable would be interacted with a measure of country-specific characteristics, it permits a direct test of whether the effect of containment measures varies across different country-specific "regimes". Second, compared with estimating structural vector autoregressions for each regime, it allows the effect of containment measures to vary smoothly across regimes by considering a continuum of states to compute impulse responses, thus making the functions more stable and precise.

Equations (1 and 2) are estimated for each day h=0,..,30. Impulse response functions are computed using the estimated coefficients θ_h, and the 90 and 95 percent confidence bands

associated with the estimated impulse-response functions are obtained using the estimated standard errors of the coefficients θ_h, based on robust standard errors clustered at the country level. Our sample consists of a balanced sample of 129 economies with at least 30 observation days after a significant outbreak (100 cases).[9]

IV. RESULTS

A. Baseline

Figure 2 shows the estimated dynamic cumulative response of the number of confirmed COVID-19 cases to a unitary change in the aggregate containment stringency index over the 30-day period following the implementation of the containment measure, together with the 90 and 95 percent confidence intervals around the point estimate. Consistent with predictions from epidemiological models, the results provide strong evidence that containment measures, by reducing mobility (Figure A1), have significantly reduced the number of infections. The magnitude of these effects is sizeable: for example, the very stringent containment measures put in place in New Zealand—restrictions on gatherings and public events implemented when cases were in single digits, followed by school and workplace closures as well as stay-at-home orders just a few days later—are likely to have reduced the number of infections by almost 90 percent relative to a baseline with no containment measures.[10] In other words, the results suggest that, in a country like New Zealand, the number of confirmed COVID-19 deaths would have been at least ten times

[9] Similar results are obtained when using alternative thresholds.

[10] The percent effects reported in the text are computed as $(e^{\theta_h}-1)*100$.

larger than in the absence of stringent containment measures. In addition, we find that lagged values of daily temperature and humidity affect significantly the number of cases and deaths, with cold and dry conditions facilitating the spread of the virus.

We also find evidence to support the hypothesis that early intervention and containment have had a significant impact on infections. For each country, we compute the public health response time (PHRT) as the number of days it takes for the country to implement containment measures after a significant outbreak (defined as 100 confirmed cases). For calculating the PHRT, we include all non-pharmaceutical interventions other than international travel restrictions, since these were often implemented before confirmed domestic outbreaks and as an effort to reduce exposure from people that had traveled to China. We find that containment measures in countries with low PHRT—that is, countries that put in place containment measures faster—reduced the average number of infections and deaths by 95, while the impact was not statistically significant for counties where the PHRT was relatively high (Figure 3).

B. Robustness checks

We carried out several robustness checks of these findings. First, since containment measures have been introduced first in China, there is the risk that the longer-term (30 days) results may simply reflect the observed flattening of the pandemic curve in China. To address this issue, we repeated the analysis excluding China from the sample. Second, we checked whether the results are driven by the inclusion of the United States, which as of now is the country with the largest number of confirmed cases and deaths. Third, instead of using an index of containment measures, which attempts to quantify the severity of the measures, we used a

simple dummy variable to identify the start and end of containment and mitigation measures—this is similar to treating the containment measures as a shock (Figure 10) . Another concern is that containment measures were announced before being implemented and, therefore, were anticipated. This may have resulted in reduced mobility ahead of the implementation of the containment measures (as shown in Figure A2) and to an upward bias in the estimates. To check for this possibility, we repeated the analysis adding changes in mobility as controls. These results are reported in Figure 4a and not statistically different from, the baseline.

Although our specification includes country specific linear, quadratic and cubic trends, it may be argued that country specific time dummies are also required, both to control for the timing of the pandemic in the global context. An additional concern is the serial correlation in the containment stringency index since the containment measures were often adopted in sequence and reversed after the number of infection has declined. Hence, we follow the methodology outlined by Teulings and Zubanov (2014) and control for leads of the stringency index— $\sum_{k=1}^{h}(\varphi_k c_{j,t+k})$ to account for containment measures introduced within the response horizon $t+h$ (for $h>1$). As reported in Figure 4b, our main results continue to hold, although there are some differences in the estimated magnitudes.

Finally, we experimented with the lag structure of the regressions, the horizon for the local projections and alternative specifications for the standard errors (e.g. Driscoll-Kraay standard errors). Our results were not affected.

C. Role of country characteristics and health infrastructure

This section examines whether the average effect of containment measures presented in the previous section varies across countries depending on country characteristics. We focus on

characteristics that are thought to influence the spread of the virus, such as the overall capacity of a country's healthcare system, its average temperature, the share of vulnerable (or elderly) persons in the population, population density, etc. Our main findings are summarized in Figure 5.

Temperature

While no strong consensus has been reached on the role of temperature in the transmission of COVID-19, emerging data as well as results discussed in the previous section suggest that cold and dry conditions may facilitate the spread of the novel coronavirus.[11] To test for the role of temperature in affecting the effect of containment measures on infections and deaths, we estimated equation (2) using the average country temperature in the first 4 months of 2020 as an interaction variable. The results in Figure 6 (top panel) suggest that the effect of containment measures was stronger in countries with lower average temperatures. While stringent containment measures may have reduced the number of confirmed cases by more about 98 percent in countries with very low average temperature, they did not have statistically significant effects in countries with very high average temperate measures. Similar results are obtained for humidity.

Age

Existing information strongly suggests that people over the age of 65 are particularly vulnerable to the effects of COVID-19. For example, in the United States about 80 percent of

[11] https://www.cebm.net/covid-19/do-weather-conditions-influence-the-transmission-of-the-coronavirus-sars-cov-2/
https://www.medrxiv.org/content/10.1101/2020.02.13.20022806v2
https://www.medrxiv.org/content/10.1101/2020.02.22.20025791v1
https://www.medrxiv.org/content/10.1101/2020.03.12.20034728v3

total deaths are concentrated in this age group.[12] The results presented in Figure 6 (bottom panel), using the share of the population above 65 as the interaction term, had a particularly large impact (reducing by about 98 percent COVID-19 cases 30 days after implementation) in countries with a relatively high share of the elderly in total population. In contrast, the impact is not statistically different from zero in countries with a very young population. The results also reflect the fact that testing has been mostly restricted to people who are most sick or hospitalized, and the elderly predominantly fall into this category.

Population density

The spread of the virus is likely to be more difficult to control in countries with higher population density, as this renders social distancing more difficult. The results in Figure 7 (top panel) confirm this hypothesis. We find that while stringent containment measures have been associated with a reduction by about 97 percent of COVID-19 cases 30 days after implementation of the measures in countries with a low population density.

Health preparedness

The preparedness and capacity of a country's health sector is of paramount importance to detect the spread of the virus and contain it. To examine whether the effect of containment measures varies according to countries' health security and capability, we estimate equation (2) using two alternative indicators of health preparedness (i) the Global Health Security Index from John Hopkins; and (ii) the Health Index compiled by the World Economic Forum. The results obtained for both indicators paint a similar picture: containment measures are more effective in countries with higher health security and a better health index (Figure 7, bottom panel and Figure

[12] https://www.cdc.gov/nchs/nvss/vsrr/covid_weekly/index.htm

A3).[13] In particular, while stringent containment measures may have reduced the number of confirmed cases by more about 97 percent in countries with very strong health systems, they did not have statistically significantly effects in countries with weak health capabilities.

Mobility and *de facto* social distancing

The analysis so far has relied on *de jure* measures of containment. However, the actual outcomes in terms of infections and deaths are likely to be determined by compliance with these *de jure* measures. In order to assess the *de facto* impact of social distancing, we interacted the containment measures with data on mobility available from Apple and Google mobility trends reports. The results suggest that containment measures have been more effective in countries where the measures resulted in *de facto* lower mobility and greater social distancing (Figure 8).

D. COVID-19 fatalities

The analysis so far has focused on the number of COVID-19 cases but can be extended to the number of confirmed COVID-19 related fatalities. While the primary role of NPIs is to slow down the rate of COVID-19 infections and ensure that the health systems are not overwhelmed, we expect a delayed effect of containment measures on the number of deaths as the reduction in the number of infections translates into lower eventual fatalities. However, an analysis of the dynamics of the number of COVID-19 related deaths is complicated by the available data as contrary to expectations, the path of confirmed cases and deaths in a given country is extremely synchronized—the average correlation between the two series in the sample is above 0.9. This is likely an artifact of the data and how confirmed cases and deaths are recorded in different

[13] Similar results are obtained for the individual sub-indices of the Global Health Security Index.

countries. Given huge uncertainty in the timing of the response of deaths to containment measures, here we focus on the total impact after 30-days as opposed to the dynamics over time.

The results presented in Figure 9 show that in addition to slowing down the number of infections, containment measures have also led to a sharp reduction in the number of COVID-19 related fatalities. Our results suggest that containment measures may have reduced the number of deaths by close to 97 percent after 30 days relative to a baseline of no containment. In addition, the country characteristics identified as playing a key role in determining the effectiveness of containment measures in reducing the number of infections also matter in limiting fatalities. If anything, factors such as population density and health infrastructure are even more important in the case of deaths.

E. Types of containment measure

In this section, we examine whether the effect of containment varies across types of measure: (i) school closures; (ii) workplace closures; (iii) cancellation of public events; (iv) restrictions on size of gathering; (v) closures of public transport; (vi) stay-at-home requirements; (vii) restrictions on internal movement; and (viii) restrictions on international travel.

Examining the effect of international travel restrictions is important to provide reassurance on the causal effect of containment measures, as such restrictions have tended to be implemented in response to outbreaks in other countries and are therefore exogenous to domestic conditions. However, estimating the effect of particular measures (other than foreign travel restrictions) is challenging, because such measures have tended to be introduced simultaneously as part of an overall strategy to limit the spread of the virus in a country.

In an attempt to overcome this challenge, we use two alternative approaches. In the first, we introduce each measure one at a time in equation (1). Clearly, the problem with this approach

is that the estimates suffer from omitted variable bias. In the second approach, we include all measures together. While this approach addresses omitted variable bias, given the high correlation across measures, the effects are likely to be less precisely estimated due to multicollinearity. The results from the two approaches suggest that all measures have contributed significantly to reducing the number of COVID-19 cases, with restrictions on international and domestic travel and stay-at-home orders appearing to have been relatively more effective in reducing the number of infections (Figure 10 and 11). The results are similar when we use dummy variables for the date of implementation or removal of the various measures (instead of the indices that quantify also the severity).

F. Re-openings and the easing of containment measures

Finally, we use more recent data for countries which have exited the lockdown phase to assess the impact of re-openings. Specifically, we look at countries which have begun easing containment measures. Such countries are identified by restricting the data to after the stringency index $c_{i,t}$ has reached its peak value and then was lowered for the remaining time frame. The sample consists of a balanced panel of 78 countries.

Figure 12 shows the estimated dynamic response of the number of confirmed COVID-19 cases to a unitary decline in the aggregate containment stringency index over the 30-day period following relaxation of the containment measure, together with 90 and 95 percent confidence intervals around the point estimate. The results suggest that relaxing containment measures have led to an increase in COVID-19 infections by more than 50 percent, relative to a baseline of stringent containment, though the results are statistically significant only at the 90 percent confidence level.

V. CONCLUSIONS

In the absence of a vaccine or effective treatments, containment measures are key to halting the spread of the virus and limiting the number of fatalities. In this paper, we have provided a first empirical assessment which quantifies the effectiveness of containment measures on the number of COVID-19 infections and deaths.

While the approach is not based on controlled experiments, our approach based on daily data and real-time observations of containment measures should limit concerns about reverse causality (from the spread of the virus to the nature of containment policies). We therefore consider our empirical estimates to provide a reasonable assessment of the causal effect of containment policies on infections. Specifically, we find that containment measures have significantly reduced the number of infections and therefore more importantly, the number of deaths. Our results suggests that countries that have put in place stringent measures, such as those implemented in Wuhan, China or in countries like New Zealand (where the stringency index has moved from about 0 to 1 in a matter of days), may have reduced the number of confirmed cases and deaths by more than 90 percent relative to the underlying country-specific path in the absence of measures.

Containment measures have had stronger effects in countries where the measures were implemented faster and resulted in less mobility—*de facto*, more social distancing—and in countries with lower temperatures, lower population density, a larger share of older population, and stronger health systems. Across different types of containment measure, internal and international travel restrictions have been most effective We also show that easing of containment measures has resulted in an increase in the number of cases, but the effect has been lower (in absolute value) than that from the tightening of measures.

References

Alesina, A.F., Furceri, D., Ostry, J.D., Papageorgiou, C. and Quinn, D.P., 2019. Structural Reforms and Elections: Evidence from a World-Wide New Dataset (No. w26720). National Bureau of Economic Research.

Auerbach, A.J. and Gorodnichenko, Y., 2013. Output spillovers from fiscal policy. American Economic Review, 103(3), pp.141-46.

Brotherhood L., Kircher P., Santos C., Tertilt M., 2020. An economic model of the COVID-19 epidemic: the importance of testing and age-specific policies. CEPR Discussion Paper DP14695, Centre for Economic Policy Research.

Chinazzi et al., 2020. The effect of travel restrictions on the spread of the 2019 novel coronavirus (COVID-19) outbreak. Science, 368, 395-400.

Cowling et al., 2020. Impact assessment of non-pharmaceutical interventions against coronavirus disease 2019 and influenza in Hong Kong: an observational study. Lancet Public Health 2020; 5: e279–88.

Eichenbaum M., Rebelo S., Trabandt M., 2020. The Macroeconomics of Epidemics. NBER Working Papers 26882, National Bureau of Economic Research, Inc.

Forslid R., Herzing M., 2020. Assessing the consequences of quarantines during a pandemic. CEPR Discussion Paper DP14699, Centre for Economic Policy Research.

Granger, C.W.J. and Teräsvirta, T., 1993. Modelling Nonlinear Economic Relationships Oxford University Press. New York.

Hsiang, S., Allen, D., Annan-Phan, S., Bell, K., Bolliger, I., Chong, T., Druckenmiller, H., Huang, L.Y., Hultgren, A., Krasovich, E. and Lau, P., 2020. The effect of large-scale anti-contagion policies on the COVID-19 pandemic. Nature, pp.1-9.

Jordà, Ò., 2005. Estimation and inference of impulse responses by local projections. American economic review, 95(1), pp.161-182.

Kraemer et al., 2020. The effect of human mobility and control measures on the COVID-19 epidemic in China. Science, 368, 493–497.

H. Tian et al., 2020. An investigation of transmission control measures during the first 50 days of the COVID-19 epidemic in China. Science10.1126/science.abb6105 (2020).

Ramey, V.A. and Zubairy, S., 2018. Government spending multipliers in good times and in bad: evidence from US historical data. Journal of Political Economy, 126(2), pp.850-901.

Teulings, Coen N., Nikolay Zubanov. 2014. “Is Economic Recovery a Myth? Robust Estimates of Impulse Responses.” *Journal of Applied Econometrics*, Vol. 29: 497-514.

Figure 1: Evolution of Total Infection and Containment Measures

Panel A. Total cases (log scale)

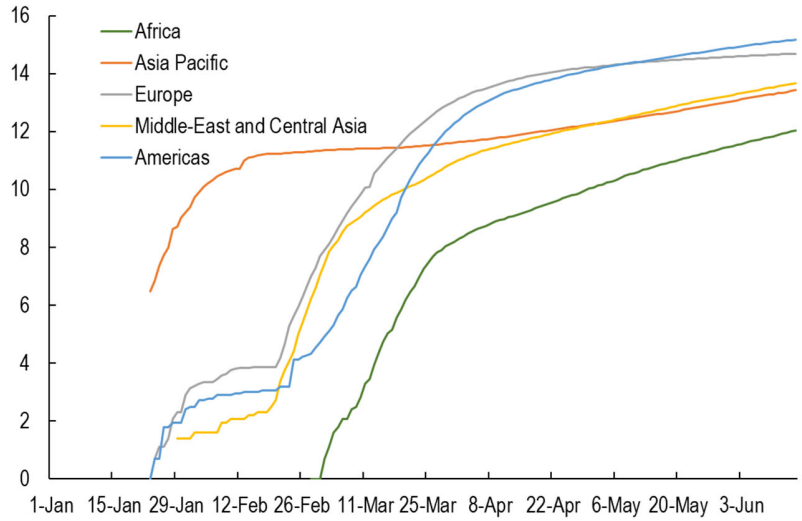

Panel B. Stringency of containment measure

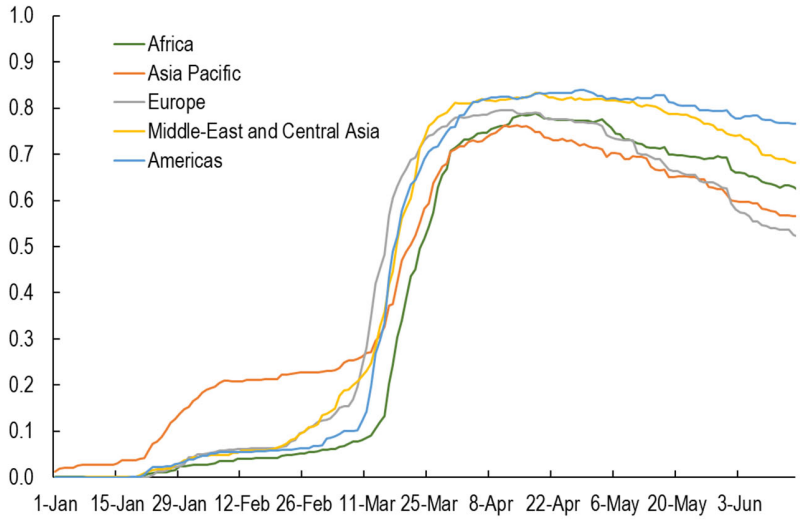

Sources: OxCGRT, and IMF staff calculations

Source: Haver, OxCGRT Stringency Index and IMF Staff calculations.
Note: The index is scaled to vary between zero (least stringent) to 1 (most stringent) containment measures. It is comprised of the following categories: (i) School closing; (ii) Workplace closing; (iii) Cancel public events; (iv) Restrictions on gathering size; (v) Close public transport; (vi) Stay at home requirements; (vii) Restrictions on internal movement; (viii) Restrictions on international travel.

Figure 2: Effect of Containment Measures on Total Confirmed COVID-19 Cases

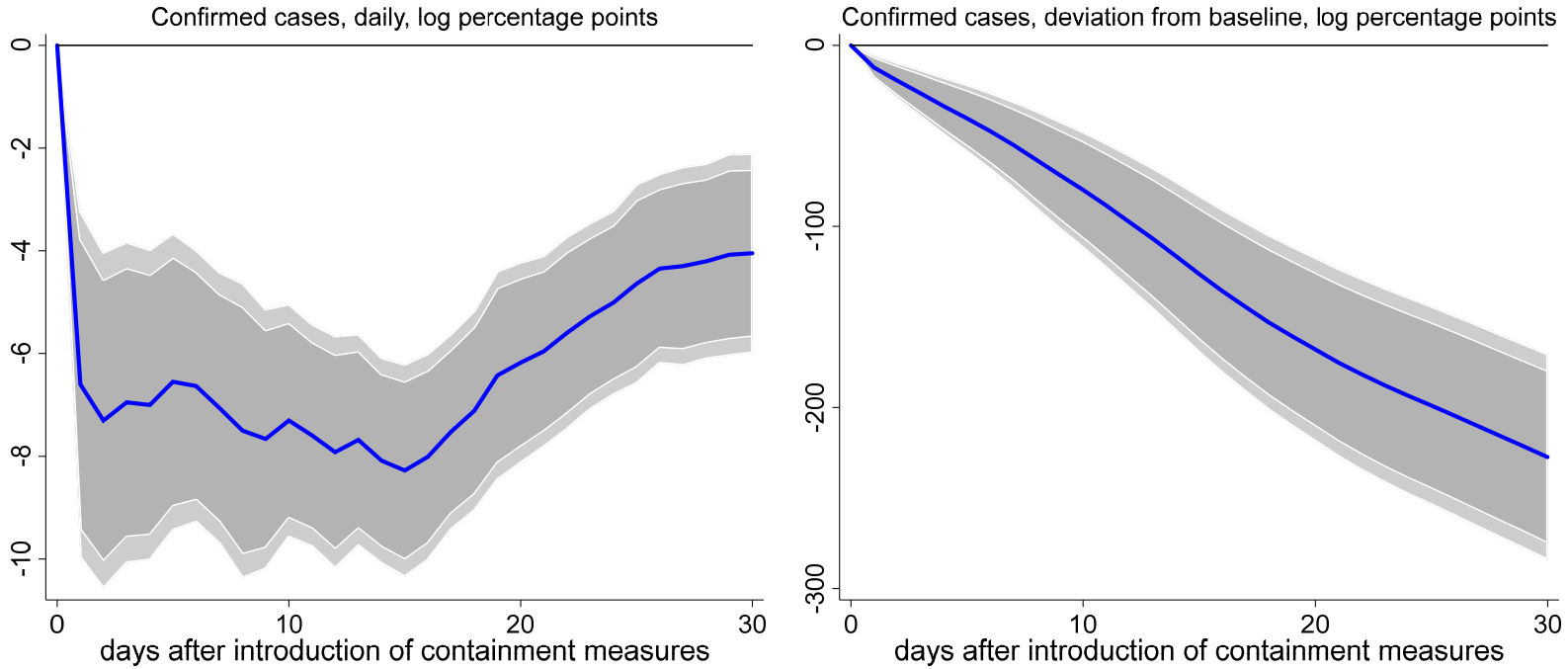

Note: Impulse response functions are estimated using a sample of 129 countries using daily data from the start of the outbreak. The analysis is restricted to countries with a significant outbreak that has lasted at least 30 days. t = 0 is the date when the outbreak becomes significant (100 cases) in each country. The graph shows the response and confidence bands at 90 and 95 percent. The horizontal axis shows the response x days after the containment measures. Estimates based on $\Delta d_{i,t+h} = u_i + \theta_h c_{i,t} + X'_{i,t}\Gamma_h + \sum_{\ell=1}^{\mathcal{L}} \psi_{h,\ell}\Delta d_{i,t-\ell} + \varepsilon_{i,t+h}$ where $\Delta d_{i,t+h} = d_{i,t+h} - d_{i,t+h-1}$ and $d_{i,t}$ is the logarithm of the number of COVID-19 cases in country i observed at date t. The model is estimated at each horizon $h = 0, 1, \ldots H$, with a lag structure $\ell = 1, 2 \ldots \mathcal{L}$; $c_{i,t}$ is the index capturing the level of containment and mitigation measures; X is a matrix of time varying control variables and country specific linear, quadratic and cubic time trend. The figure displays log-difference changes whereas the text translates these into percent changes. Results are based on June 15 data.

Figure 3: Interaction with Public Health Response Time

(deviation from baseline, log percentage points)

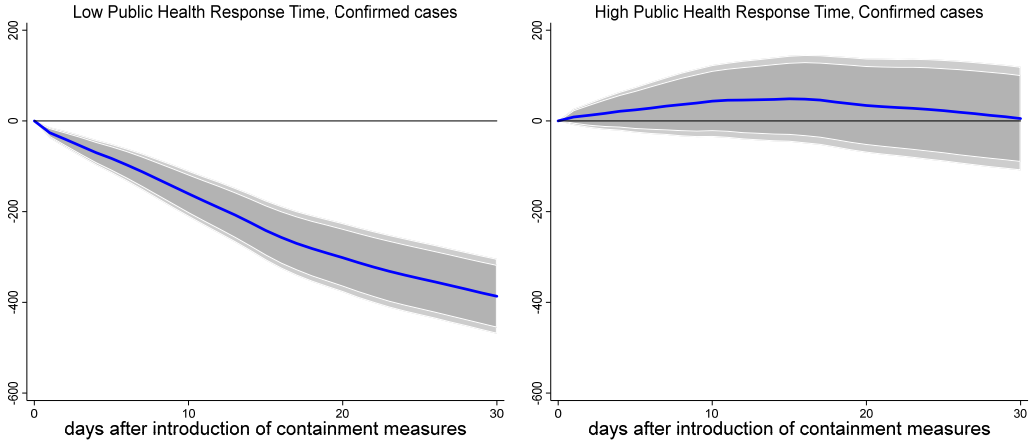

Note: Impulse response functions are estimated using a sample of 129 countries using daily data from the start of the outbreak. The analysis is restricted to countries with a significant outbreak that has lasted at least 30 days. The graph shows the response and confidence bands at 90 and 95 percent. The horizontal axis shows the response x days after the containment measures. Estimates based on $\Delta d_{i,t+h} = u_i + u_t + \theta_h^L F(z_{i,t}) c_{i,t} + \theta_h^H (1 - F(z_{i,t})) c_{i,t} + X'_{i,t}\Gamma_h + \sum_{\ell=1}^{\mathcal{L}} F(z_{i,t})\, \psi_{h,\ell} \Delta d_{i,t-\ell} + \sum_{\ell=1}^{\mathcal{L}} (1 - F(z_{i,t}))\psi_{h,\ell} \Delta d_{i,t-\ell} + \varepsilon_{i,t+h}$ with $F(z_{it}) = \frac{exp^{-\gamma z_{it}}}{(1-exp^{-\gamma z_{it}})}, \gamma > 0$ where $\Delta d_{i,t+h} = d_{i,t+h} - d_{i,t+h-1}$ and $d_{i,t}$ is the logarithm of the number of COVID-19 cases in country i observed at date t and z is the country-specific characteristics normalized to have zero mean and a unit variance. The model is estimated at each horizon $h = 0, 1, \ldots H$, with a lag structure $\ell = 1, 2 \ldots \mathcal{L}$; $c_{i,t}$ is the index capturing the level of containment and mitigation measures; X is a matrix of time varying control variables and country specific linear, quadratic and cubic time trend. Results are based on June 15 data. The figure displays log-difference changes whereas the text translates these into percent changes.

Figure 4a: Robustness Checks

Response to stringency of containment measures: ex China

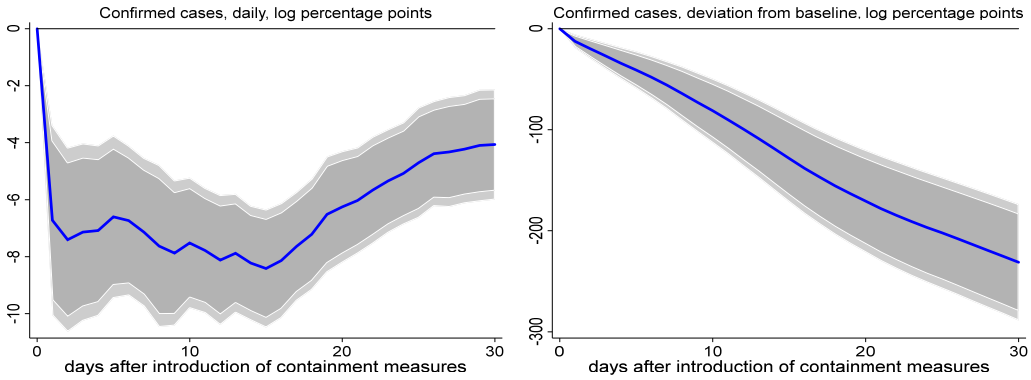

Response to stringency of containment measures: ex US

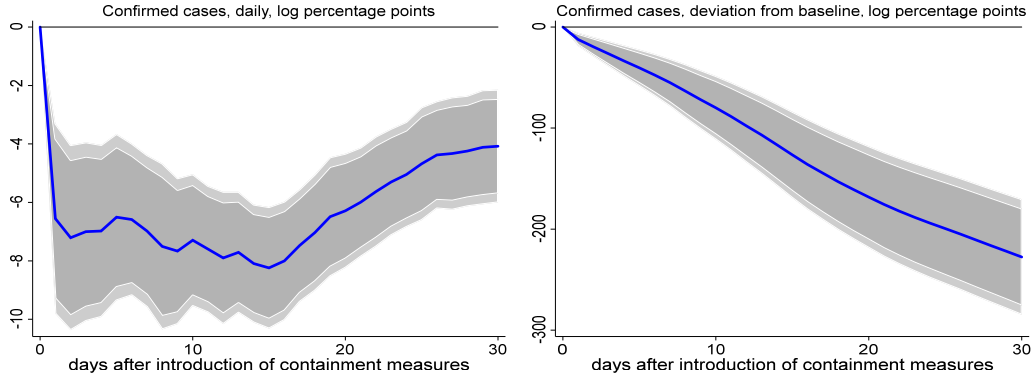

Response to stringency of containment measures: with mobility controls

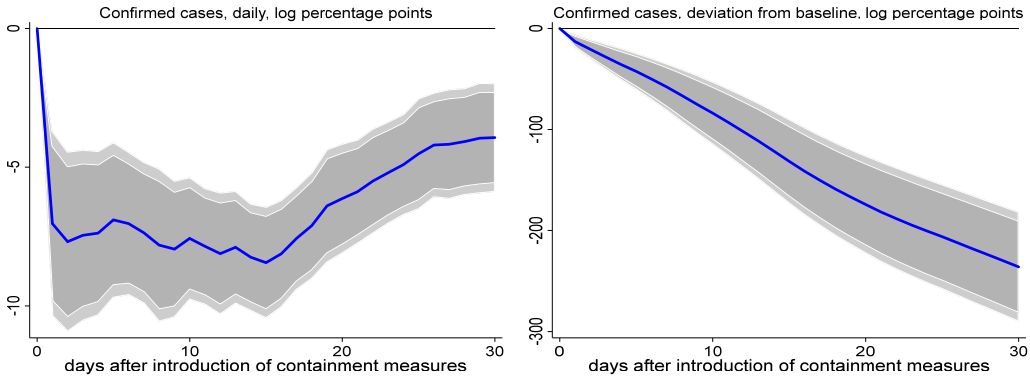

Note: Impulse response functions are estimated using a sample of 129 countries using daily data from the start of the outbreak. The analysis is restricted to countries with a significant outbreak that has lasted at least 30 days. t = 0 is the date when the outbreak becomes significant (100 cases) in each country. The graph shows the response and confidence bands at 90 and 95 percent. The horizontal axis shows the response x days after the containment measures. Estimates based on $\Delta d_{i,t+h} = u_i + \theta_h c_{i,t} + X'_{i,t}\Gamma_h + \sum_{\ell=1}^{\mathcal{L}} \psi_{h,\ell}\Delta d_{i,t-\ell} + \varepsilon_{i,t+h}$ where $\Delta d_{i,t+h} = d_{i,t+h} - d_{i,t+h-1}$ and $d_{i,t}$ is the logarithm of the number of COVID-19 cases in country i observed at date t. The model is estimated at each horizon $h = 0, 1, \ldots H$, with a lag structure $\ell = 1, 2 \ldots \mathcal{L}$; $c_{i,t}$ is the index capturing the level of containment and mitigation measures; X is a matrix of time varying control variables and country specific linear, quadratic and cubic time trend. Results are based on June 15 data. The figure displays log-difference changes whereas the text translates these into percent changes.

Figure 4b: Robustness Checks

Response to stringency of containment measures: with time fixed effects

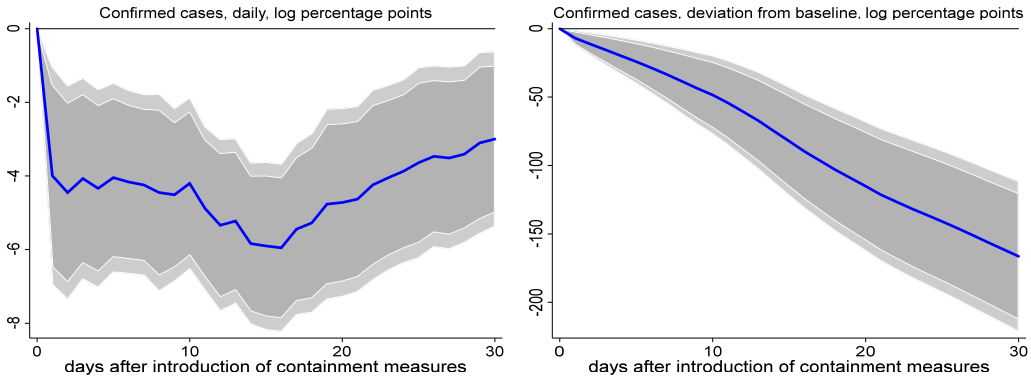

Response to stringency of containment measures: additional controls for serial correlation of measures (leads)

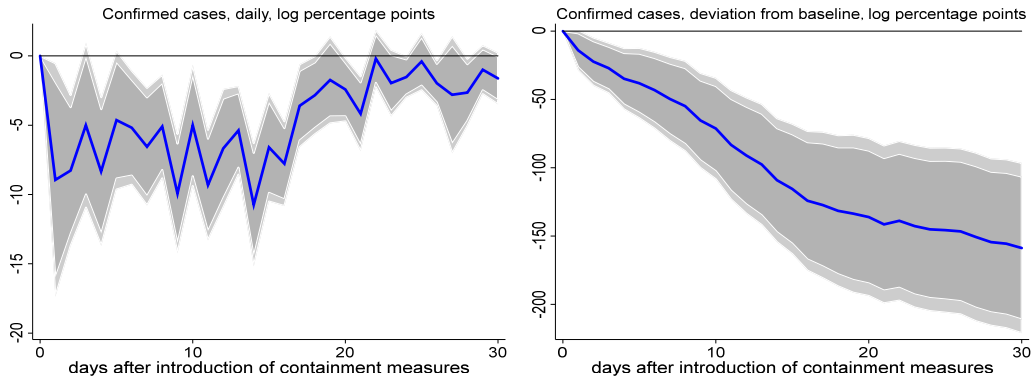

Response to stringency of containment measures: with time fixed effects and leads

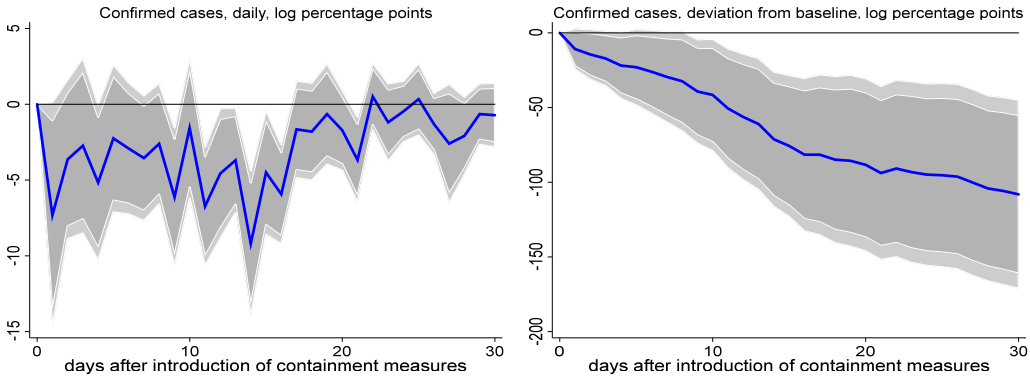

Note: Impulse response functions are estimated using a sample of 129 countries using daily data from the start of the outbreak. The analysis is restricted to countries with a significant outbreak that has lasted at least 30 days. t = 0 is the date when the outbreak becomes significant (100 cases) in each country. The graph shows the response and confidence bands at 90 and 95 percent. The horizontal axis shows the response x days after the containment measures. Estimates based on $\Delta d_{i,t+h} = u_i + \theta_h c_{i,t} + X'_{i,t}\Gamma_h + \sum_{\ell=1}^{\mathcal{L}} \psi_{h,\ell}\Delta d_{i,t-\ell} + \varepsilon_{i,t+h}$ where $\Delta d_{i,t+h} = d_{i,t+h} - d_{i,t+h-1}$ and $d_{i,t}$ is the logarithm of the number of COVID-19 cases in country i observed at date t. The model is estimated at each horizon $h = 0, 1, \ldots H$, with a lag structure $\ell = 1, 2 \ldots \mathcal{L}$; $c_{i,t}$ is the index capturing the level of containment and mitigation measures; X is a matrix of time varying control variables and country specific linear, quadratic and cubic time trend. The last two panels add leads of the containment measure, $\sum_{k=1}^{h}(\varphi_k c_{i,t+k})$, to account for containment measures introduced during the response horizon. Results are based on June 15 data. The figure displays log-difference changes whereas the text translates these into percent changes.

Figure 5: Summary of interactions with country characteristics

(percent deviation from baseline 30 days after the introduction of containment measures)

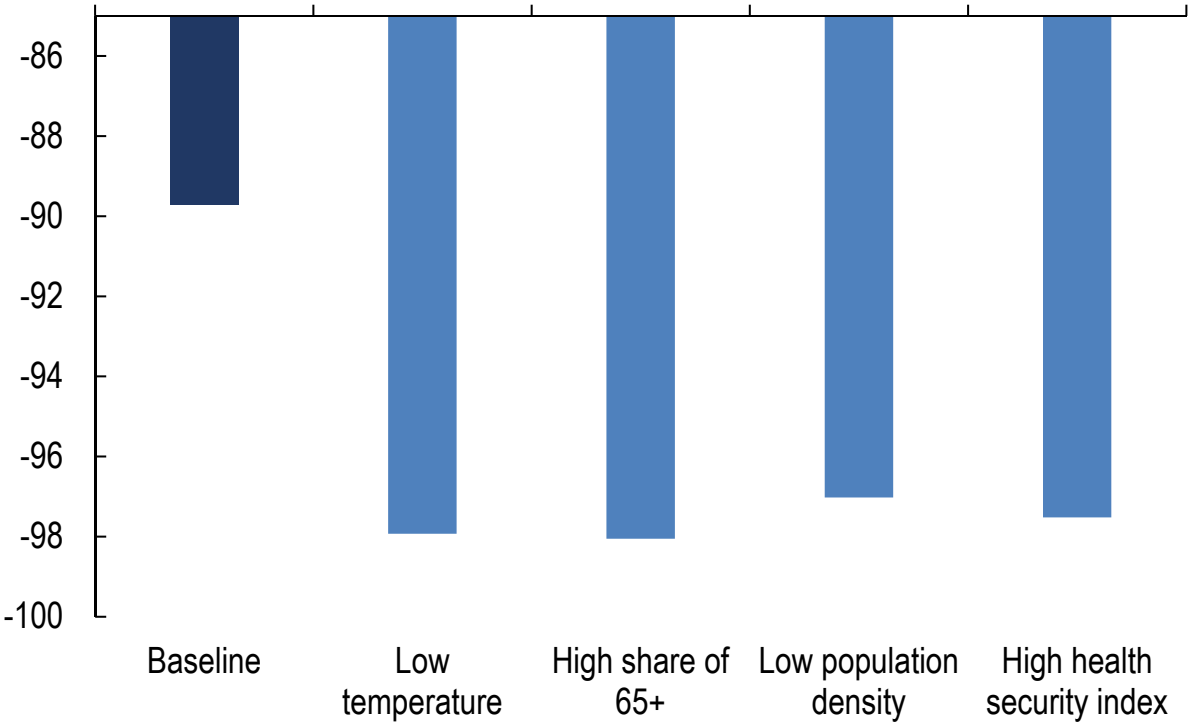

Note: Impulse response functions are estimated using a sample of 129 countries using daily data from the start of the outbreak. The analysis is restricted to countries with a significant outbreak that has lasted at least 30 days. The graph shows the cumulative response after 30 days for beeline and each county characteristic. Estimates based on $\Delta d_{i,t+h} = u_i + u_t + \theta_h^L F(z_{i,t}) c_{i,t} + \theta_h^H (1 - F(z_{i,t})) c_{i,t} + X'_{i,t}\Gamma_h + \sum_{\ell=1}^{\mathcal{L}} F(z_{i,t})\, \psi_{h,\ell} \Delta d_{i,t-\ell} + \sum_{\ell=1}^{\mathcal{L}} (1 - F(z_{i,t})) \psi_{h,\ell} \Delta d_{i,t-\ell} + \varepsilon_{i,t+h}$ with $F(z_{it}) = \frac{exp^{-\gamma z_{it}}}{(1-exp^{-\gamma z_{it}})}, \gamma > 0$ where $\Delta d_{i,t+h} = d_{i,t+h} - d_{i,t+h-1}$ and $d_{i,t}$ is the logarithm of the number of COVID-19 cases in country i observed at date t and z is the country-specific characteristics normalized to have zero mean and a unit variance. The model is estimated at each horizon $h = 0, 1, \ldots H$, with a lag structure $\ell = 1, 2 \ldots \mathcal{L}$; $c_{i,t}$ is the index capturing the level of containment and mitigation measures; X is a matrix of time varying control variables and country specific linear, quadratic and cubic time trend. Results are based on June 15 data.

Figure 6: Interaction with Temperature and Elderly Population

(deviation from baseline, log percentage points)

Average Air Temperature

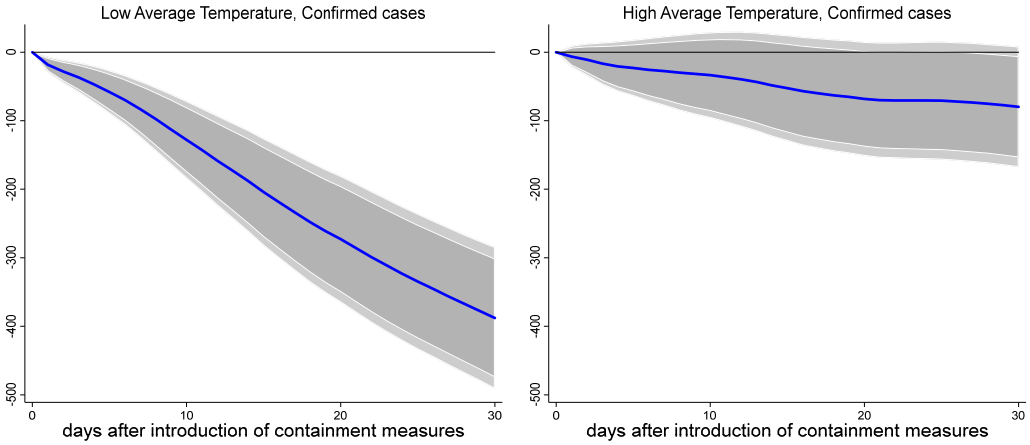

Share of Population above 65 years

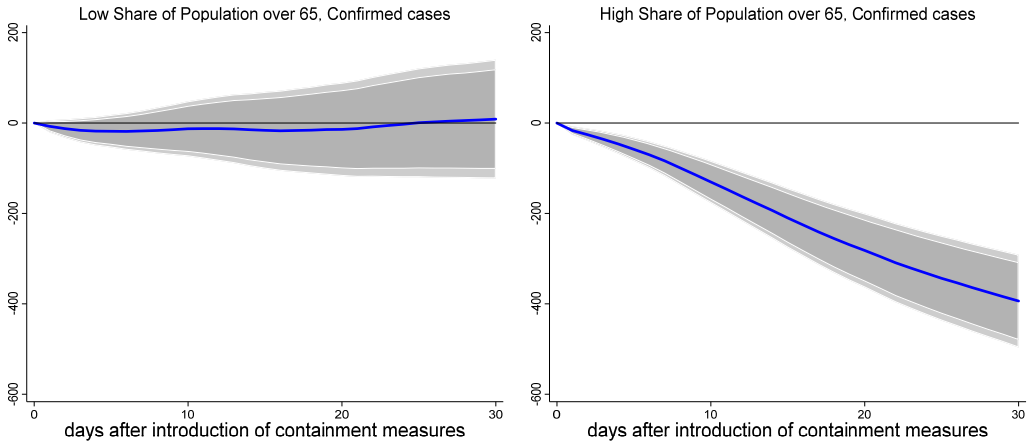

Note: Impulse response functions are estimated using a sample of 129 countries using daily data from the start of the outbreak. The analysis is restricted to countries with a significant outbreak that has lasted at least 30 days. The graph shows the response and confidence bands at 90 and 95 percent. The horizontal axis shows the response x days after the containment measures. Estimates based on $\Delta d_{i,t+h} = u_i + u_t + \theta_h^L F(z_{i,t}) c_{i,t} + \theta_h^H (1 - F(z_{i,t})) c_{i,t} + X'_{i,t}\Gamma_h + \sum_{\ell=1}^{\mathcal{L}} F(z_{i,t})\, \psi_{h,\ell} \Delta d_{i,t-\ell} + \sum_{\ell=1}^{\mathcal{L}} (1 - F(z_{i,t}))\psi_{h,\ell} \Delta d_{i,t-\ell} + \varepsilon_{i,t+h}$ with $F(z_{it}) = \frac{exp^{-\gamma z_{it}}}{(1-exp^{-\gamma z_{it}})}, \gamma > 0$ where $\Delta d_{i,t+h} = d_{i,t+h} - d_{i,t+h-1}$ and $d_{i,t}$ is the logarithm of the number of COVID-19 cases in country i observed at date t and z is the country-specific characteristics normalized to have zero mean and a unit variance. The model is estimated at each horizon $h = 0, 1, \ldots H$, with a lag structure $\ell = 1, 2 \ldots \mathcal{L}$; $c_{i,t}$ is the index capturing the level of containment and mitigation measures; X is a matrix of time varying control variables and country specific linear, quadratic and cubic time trend. Results are based on June 15 data. The figure displays log-difference changes whereas the text translates these into percent changes.

Figure 7: Interaction with Population Density and Health Infrastructure

(deviation from baseline, log percentage points)

Population Density

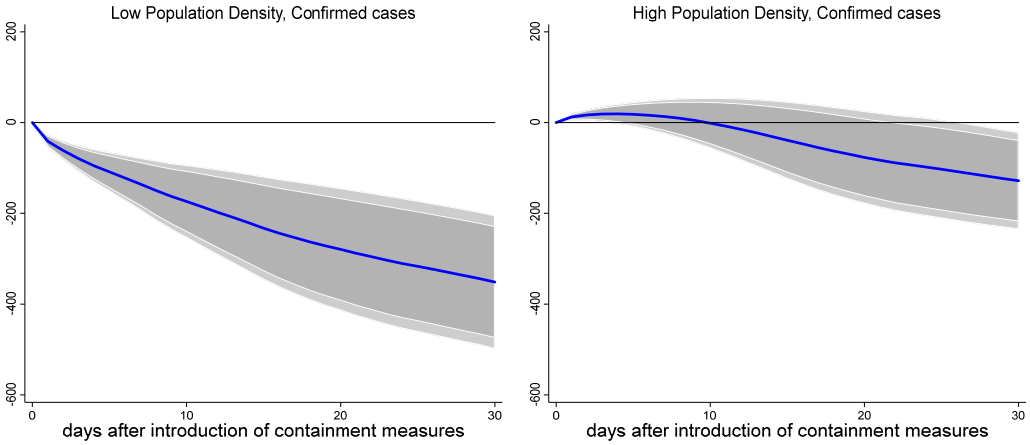

Health Security Index

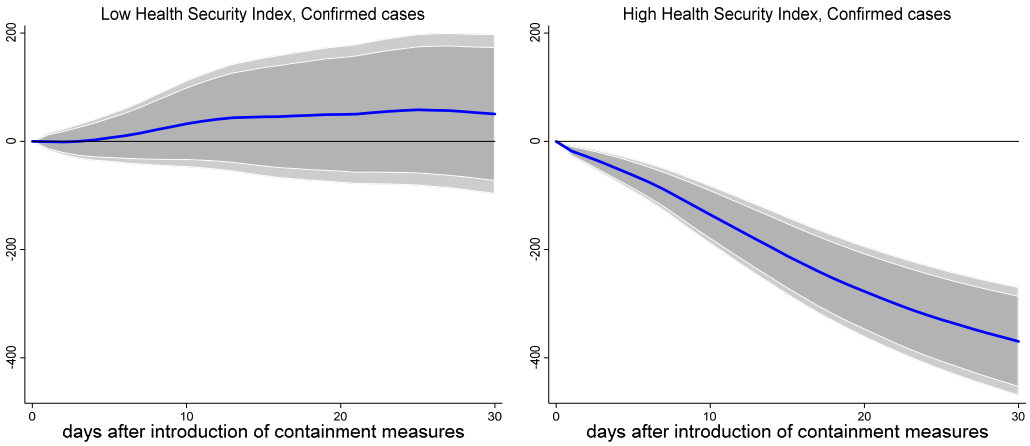

Note: Impulse response functions are estimated using a sample of 129 countries using daily data from the start of the outbreak. The analysis is restricted to countries with a significant outbreak that has lasted at least 30 days. The graph shows the response and confidence bands at 90 and 95 percent. The horizontal axis shows the response x days after the containment measures. Estimates based on $\Delta d_{i,t+h} = u_i + u_t + \theta_h^L F(z_{i,t}) c_{i,t} + \theta_h^H (1 - F(z_{i,t})) c_{i,t} + X'_{i,t}\Gamma_h + \sum_{\ell=1}^{\mathcal{L}} F(z_{i,t})\, \psi_{h,\ell} \Delta d_{i,t-\ell} + \sum_{\ell=1}^{\mathcal{L}} (1 - F(z_{i,t}))\psi_{h,\ell} \Delta d_{i,t-\ell} + \varepsilon_{i,t+h}$ with $F(z_{it}) = \frac{exp^{-\gamma z_{it}}}{(1-exp^{-\gamma z_{it}})}, \gamma > 0$ where $\Delta d_{i,t+h} = d_{i,t+h} - d_{i,t+h-1}$ and $d_{i,t}$ is the logarithm of the number of COVID-19 cases in country i observed at date t and z is the country-specific characteristics normalized to have zero mean and a unit variance. The model is estimated at each horizon $h = 0, 1, \ldots H$, with a lag structure $\ell = 1, 2 \ldots \mathcal{L}$; $c_{i,t}$ is the index capturing the level of containment and mitigation measures; X is a matrix of time varying control variables and country specific linear, quadratic and cubic time trend. Results are based on June 15 data. The figure displays log-difference changes whereas the text translates these into percent changes.

Figure 8: Interaction with Mobility

(deviation from baseline, log percentage points)

Driving Mobility (Apple)

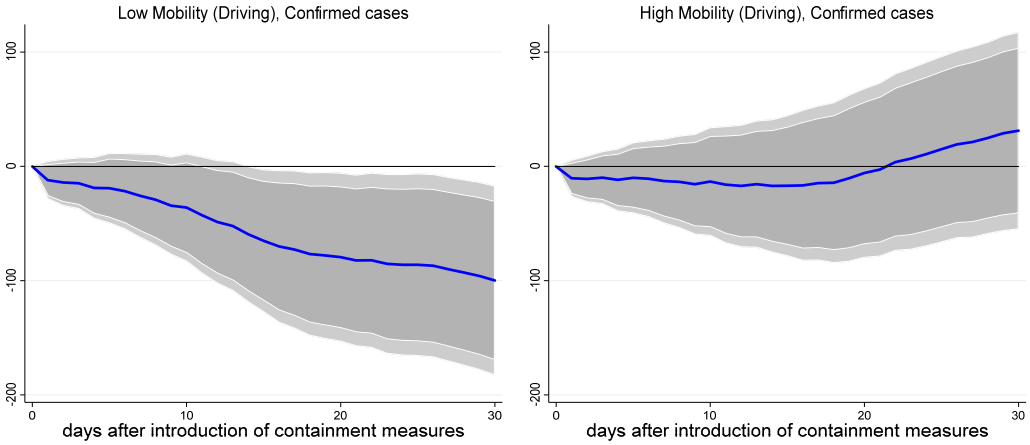

Retail Mobility (Google)

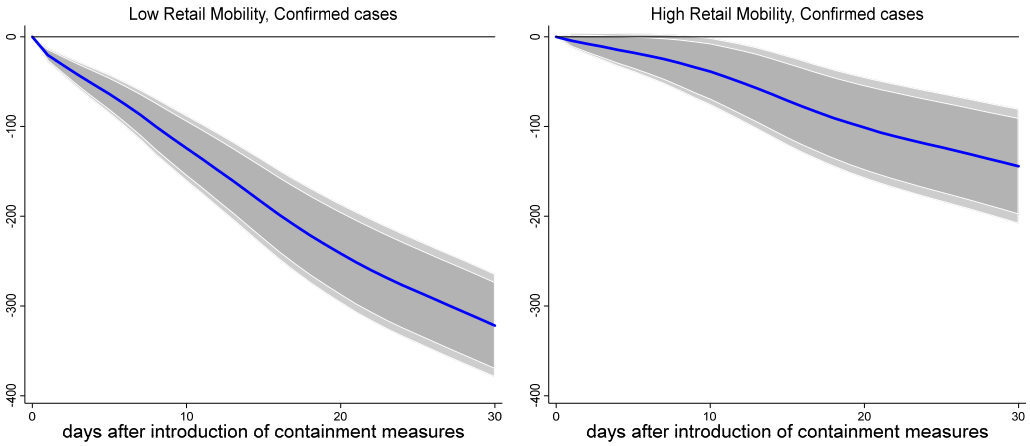

Note: Impulse response functions are estimated using a sample of 129 countries using daily data from the start of the outbreak. The analysis is restricted to countries with a significant outbreak that has lasted at least 30 days. The graph shows the response and confidence bands at 90 and 95 percent. The horizontal axis shows the response x days after the containment measures. Estimates based on $\Delta d_{i,t+h} = u_i + u_t + \theta_h^L F(z_{i,t}) c_{i,t} + \theta_h^H (1 - F(z_{i,t})) c_{i,t} + X'_{i,t}\Gamma_h + \sum_{\ell=1}^{\mathcal{L}} F(z_{i,t})\, \psi_{h,\ell} \Delta d_{i,t-\ell} + \sum_{\ell=1}^{\mathcal{L}} (1 - F(z_{i,t}))\psi_{h,\ell} \Delta d_{i,t-\ell} + \varepsilon_{i,t+h}$ with $F(z_{it}) = \frac{exp^{-\gamma z_{it}}}{(1-exp^{-\gamma z_{it}})}, \gamma > 0$ where $\Delta d_{i,t+h} = d_{i,t+h} - d_{i,t+h-1}$ and $d_{i,t}$ is the logarithm of the number of COVID-19 cases in country i observed at date t and z is the country-specific characteristics normalized to have zero mean and a unit variance. The model is estimated at each horizon $h = 0, 1, \ldots H$, with a lag structure $\ell = 1, 2 \ldots \mathcal{L}$; $c_{i,t}$ is the index capturing the level of containment and mitigation measures; X is a matrix of time varying control variables and country specific linear, quadratic and cubic time trend. Results are based on June 15 data. The figure displays log-difference changes whereas the text translates these into percent changes.

Figure 9: Effect of Containment Measures on Total Confirmed COVID-19 Deaths

(percent deviation from baseline 30 days after the introduction of containment measures)

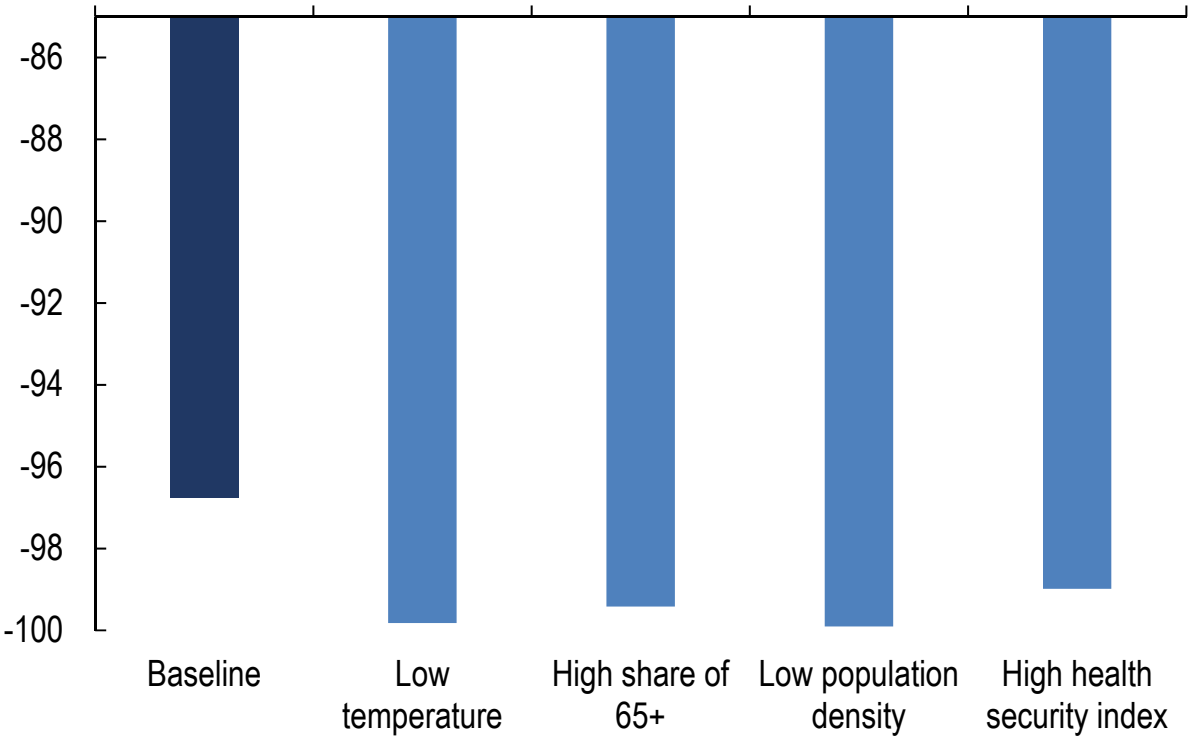

Note: Impulse response functions are estimated using a sample of 129 countries using daily data from the start of the outbreak. The analysis is restricted to countries with a significant outbreak that has lasted at least 30 days. The graph shows the cumulative response after 30 days for beeline and each county characteristic. Estimates based on $\Delta d_{i,t+h} = u_i + u_t + \theta_h^L F(z_{i,t}) c_{i,t} + \theta_h^H (1 - F(z_{i,t})) c_{i,t} + X'_{i,t}\Gamma_h + \sum_{\ell=1}^{\mathcal{L}} F(z_{i,t})\, \psi_{h,\ell} \Delta d_{i,t-\ell} + \sum_{\ell=1}^{\mathcal{L}} (1 - F(z_{i,t})) \psi_{h,\ell} \Delta d_{i,t-\ell} + \varepsilon_{i,t+h}$ with $F(z_{it}) = \frac{exp^{-\gamma z_{it}}}{(1-exp^{-\gamma z_{it}})}, \gamma > 0$ where $\Delta d_{i,t+h} = d_{i,t+h} - d_{i,t+h-1}$ and $d_{i,t}$ is the logarithm of the number of COVID-19 deaths in country i observed at date t and z is the country-specific characteristics normalized to have zero mean and a unit variance. The model is estimated at each horizon $h = 0, 1, \ldots H$, with a lag structure $\ell = 1, 2 \ldots \mathcal{L}$; $c_{i,t}$ is the index capturing the level of containment and mitigation measures; X is a matrix of time varying control variables and country specific linear, quadratic and cubic time trend. Results are based on June 15 data.

Figure 10: Local projection response to different containment measures

(deviation from baseline, log percentage points)

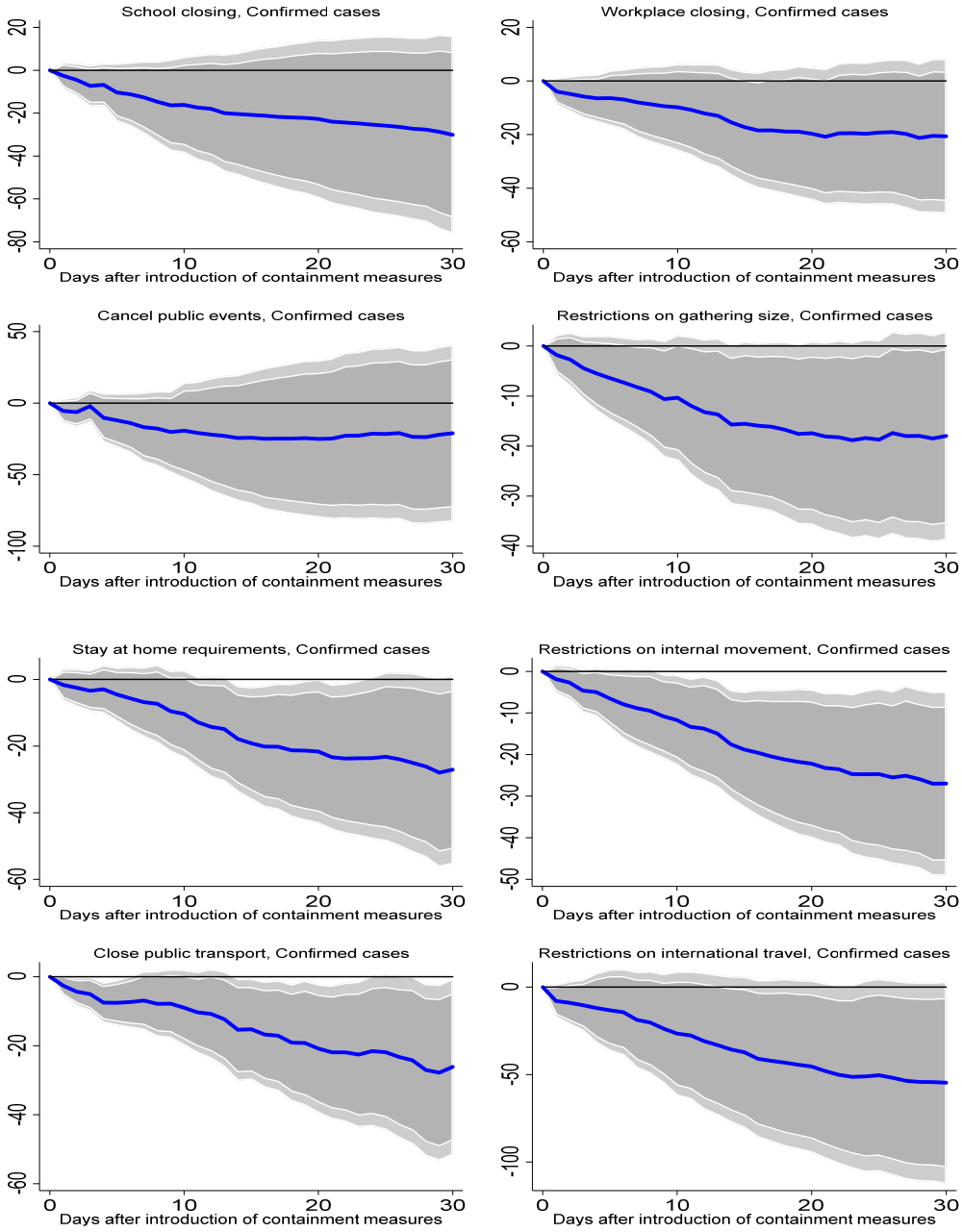

Note: Impulse response functions are estimated using a sample of 129 countries using daily data from the start of the outbreak. The analysis is restricted to countries with a significant outbreak that has lasted at least 30 days. t = 0 is the date when the outbreak becomes significant (100 cases) in each country. The graph shows the response and confidence bands at 90 and 95 percent. The horizontal axis shows the response x days after the containment measures. Estimates based on $\Delta d_{i,t+h} = u_i + \theta_h c_{i,t} + X'_{i,t}\Gamma_h + \sum_{\ell=1}^{\mathcal{L}} \psi_{h,\ell}\Delta d_{i,t-\ell} + \varepsilon_{i,t+h}$ where $\Delta d_{i,t+h} = d_{i,t+h} - d_{i,t+h-1}$ and $d_{i,t}$ is the logarithm of the number of COVID-19 cases in country i observed at date t. The model is estimated at each horizon $h = 0, 1, \ldots H$, with a lag structure $\ell = 1, 2 \ldots \mathcal{L}$; $c_{i,t}$ is the index capturing different types containment and mitigation measures, introduced one at a time; X is a matrix of time varying control variables and country specific linear, quadratic and cubic time trend. Results are based on June 15 data. The figure displays log-difference changes whereas the text translates these into percent changes.

Figure 11: Local projection response to different containment measures (together)

(deviation from baseline, log percentage points)

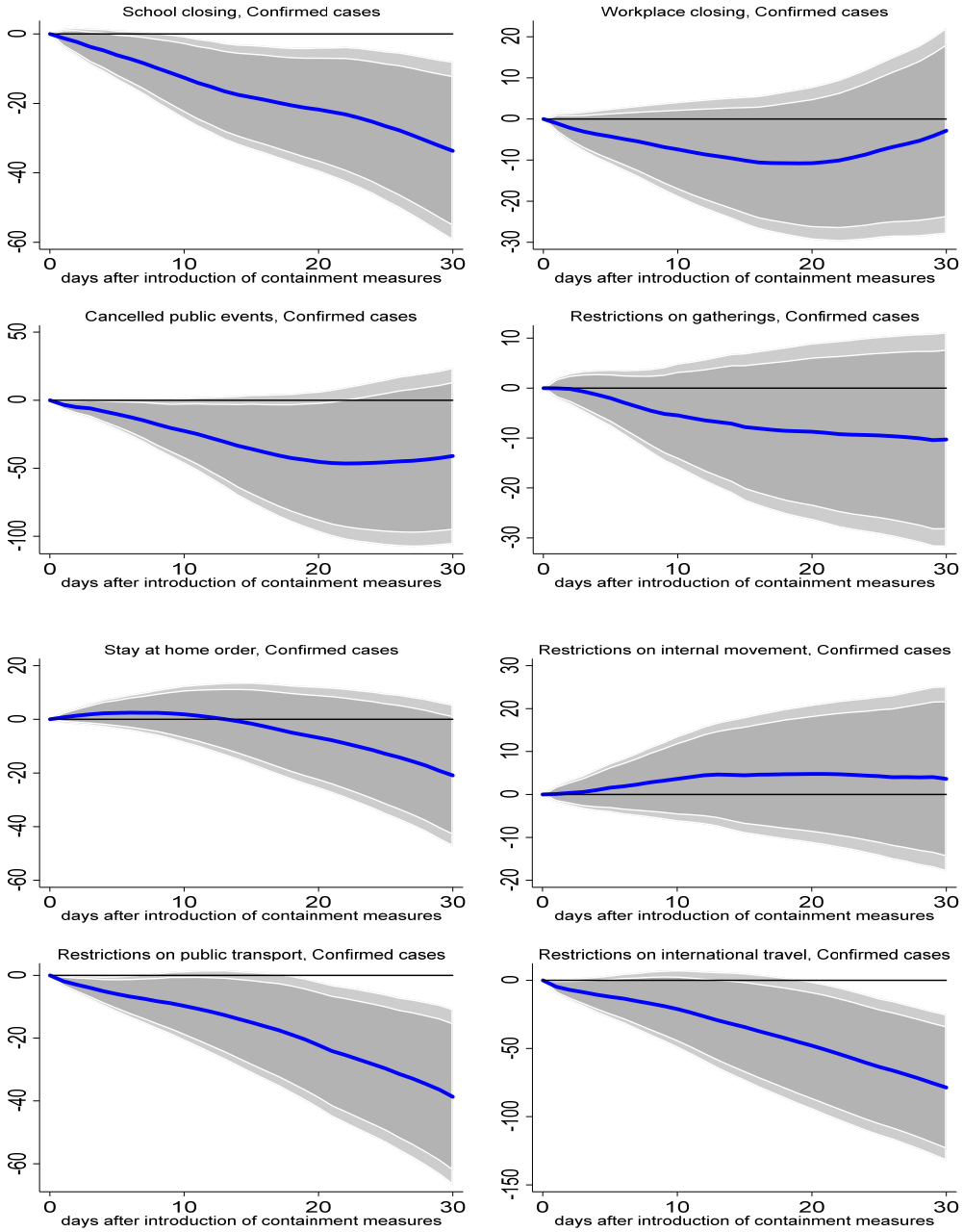

Note: Impulse response functions are estimated using a sample of 129 countries using daily data from the start of the outbreak. The analysis is restricted to countries with a significant outbreak that has lasted at least 30 days. t = 0 is the date when the outbreak becomes significant (100 cases) in each country. The graph shows the response and confidence bands at 95 percent. The horizontal axis shows the response x days after the containment measures. Estimates based on $\Delta d_{i,t+h} = u_i + \theta_h c_{i,t} + X'_{i,t}\Gamma_h + \sum_{\ell=1}^{\mathcal{L}} \psi_{h,\ell} \Delta d_{i,t-\ell} + \sum_{k=1}^{h} (\varphi_k c_{i,t+k}) + \varepsilon_{i,t+h}$ where $\Delta d_{i,t+h} = d_{i,t+h} - d_{i,t+h-1}$ and $d_{i,t}$ is the logarithm of the number of COVID-19 cases or deaths (depending on specification) in country i observed at date t. The model is estimated at each horizon $h = 0, 1, \ldots H$, with a lag structure $\ell = 1, 2 \ldots \mathcal{L}$; $c_{i,t}$ are indices capturing different types containment and mitigation measures, introduced simultaneously in the regression; X is a matrix of time varying control variables and country specific linear, quadratic and cubic time trend. Results are based on June 15 data. The figure displays log-difference changes whereas the text translates these into percent changes.

Figure 12: Effect of Containment Measures on Total Confirmed COVID-19 Cases

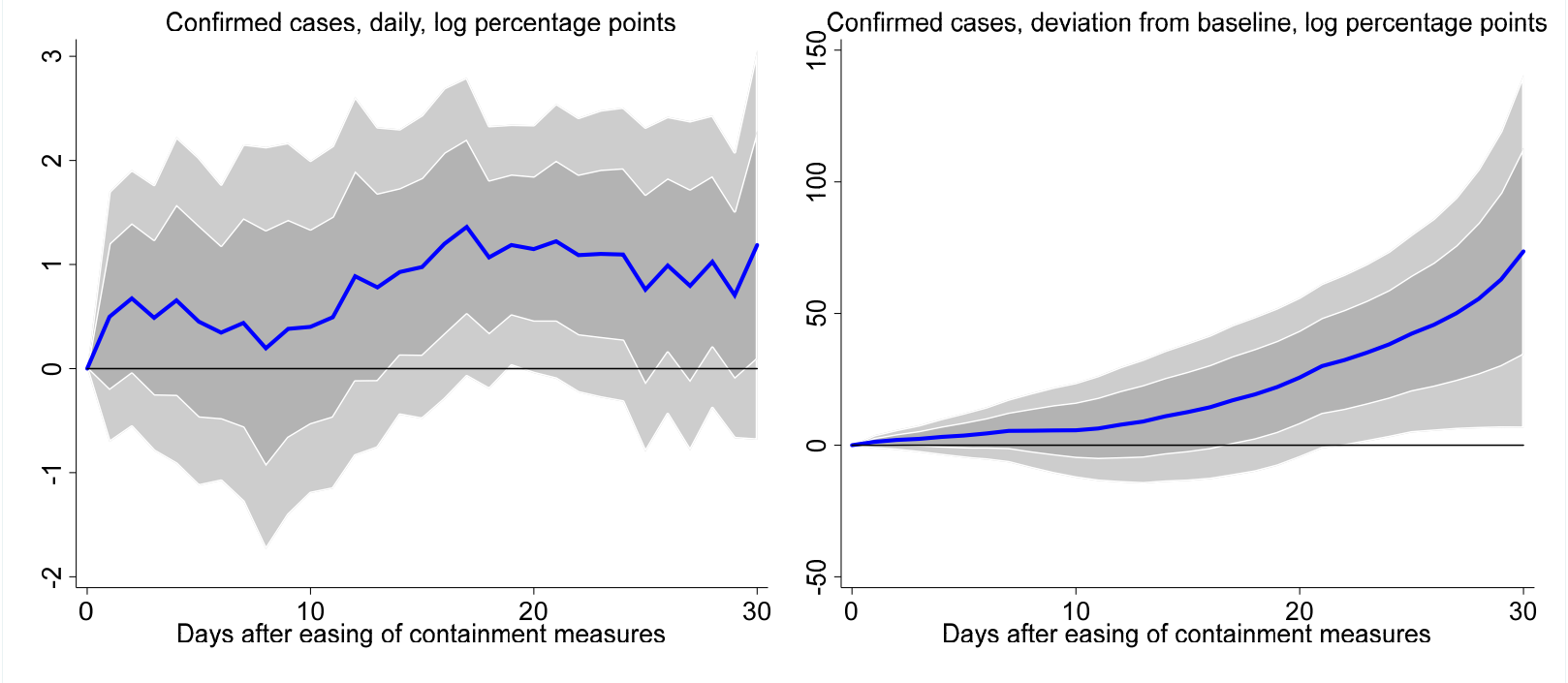

Note: Impulse response functions are estimated using a sample of 129 countries using daily data from the start of the outbreak. The analysis is restricted to countries with a significant outbreak that has lasted at least 30 days. t = 0 is the date when the outbreak becomes significant (100 cases) in each country. The graph shows the response and confidence bands at 90 and 95 percent. The horizontal axis shows the response x days after the easing of containment measures. Estimates based on $\Delta d_{i,t+h} = u_i + \theta_h c_{i,t} + X'_{i,t}\Gamma_h + \sum_{\ell=1}^{\mathcal{L}} \psi_{h,\ell}\Delta d_{i,t-\ell} + \varepsilon_{i,t+h}$ where $\Delta d_{i,t+h} = d_{i,t+h} - d_{i,t+h-1}$ and $d_{i,t}$ is the logarithm of the number of COVID-19 cases in country i observed at date t. The model is estimated at each horizon $h = 0, 1, \ldots H$, with a lag structure $\ell = 1, 2 \ldots \mathcal{L}$; $c_{i,t}$ is the index capturing the level of containment and mitigation measures; X is a matrix of time varying control variables and country specific linear, quadratic and cubic time trend. The figure displays log-difference changes whereas the text translates these into percent changes. Results are based on June 15 data.

ANNEX

Figure A1: Effect of Containment Measures on Mobility

(deviation from baseline, log percentage points)

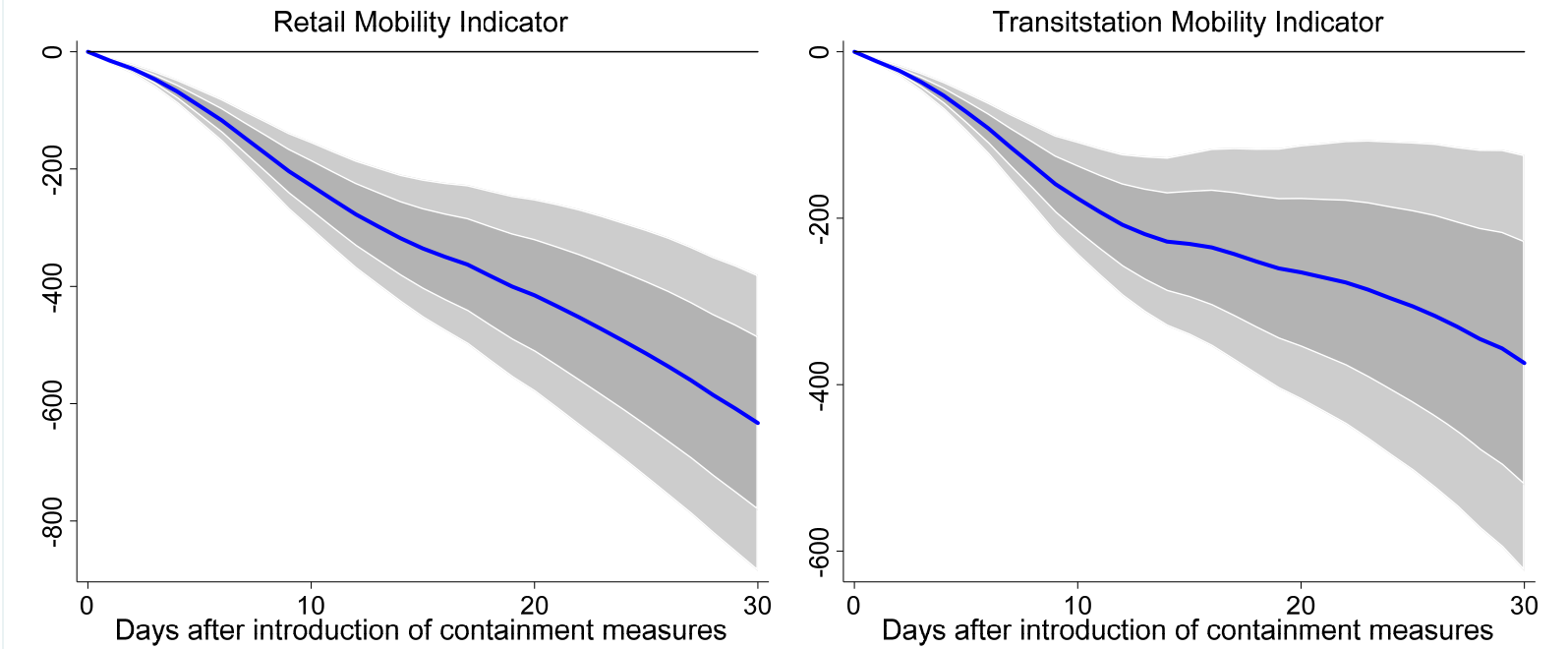

Note: Impulse response functions are estimated using a sample of 70 countries using daily data from the start of the outbreak. Google mobility and retail indices are reported as percent deviations for each day of the week to that corresponding day of the week in the baseline. They are smoothed out over 7 days to estimate the average deviation from the baseline, and then cumulated to report the total deviation from the baseline. The analysis is restricted to countries with a significant outbreak that has lasted at least 30 days. t = 0 is the date when the outbreak becomes significant (100 cases) in each country. The graph shows the response and confidence bands at 95 percent. The horizontal axis shows the response x days after the containment measures. Estimates based on $\Delta d_{i,t+h} = u_i + \theta_h c_{i,t} + X'_{i,t}\Gamma_h + \sum_{\ell=1}^{\mathcal{L}} \psi_{h,\ell} \Delta d_{i,t-\ell} + \sum_{k=1}^{h} (\varphi_k c_{i,t+k}) + \varepsilon_{i,t+h}$ where $\Delta d_{i,t+h} = d_{i,t+h} - d_{i,t+h-1}$ and $d_{i,t}$ is the logarithm mobility in country i observed at date t. The model is estimated at each horizon $h = 0, 1, \ldots H$, with a lag structure $\ell = 1, 2 \ldots \mathcal{L}$; $c_{i,t}$ is the index capturing the level of containment and mitigation measures; X is a matrix of time varying control variables and country specific linear, quadratic and cubic time trend. Results are based on June 15 data.

Figure A2: Containment measures and mobility

(mobility index, percent)

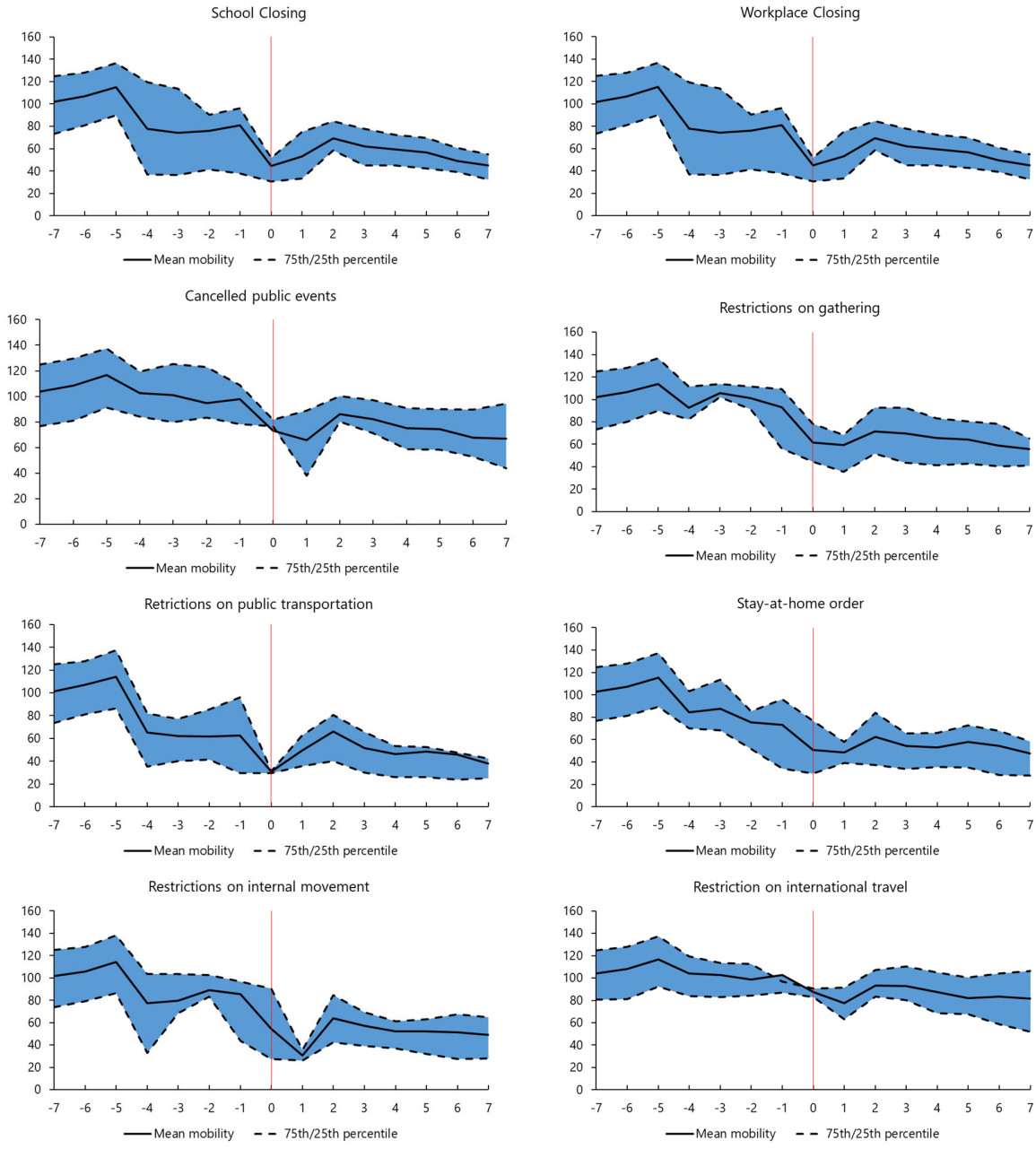

Sources: Apple Mobility Indices, OxCGRT Stringency Index and IMF Staff calculations. An index =100 suggest no decline in mobility compared to trends.

Figure A3: Interaction with Health Security Index and Health Infrastructure

(deviation from baseline, log percentage points)

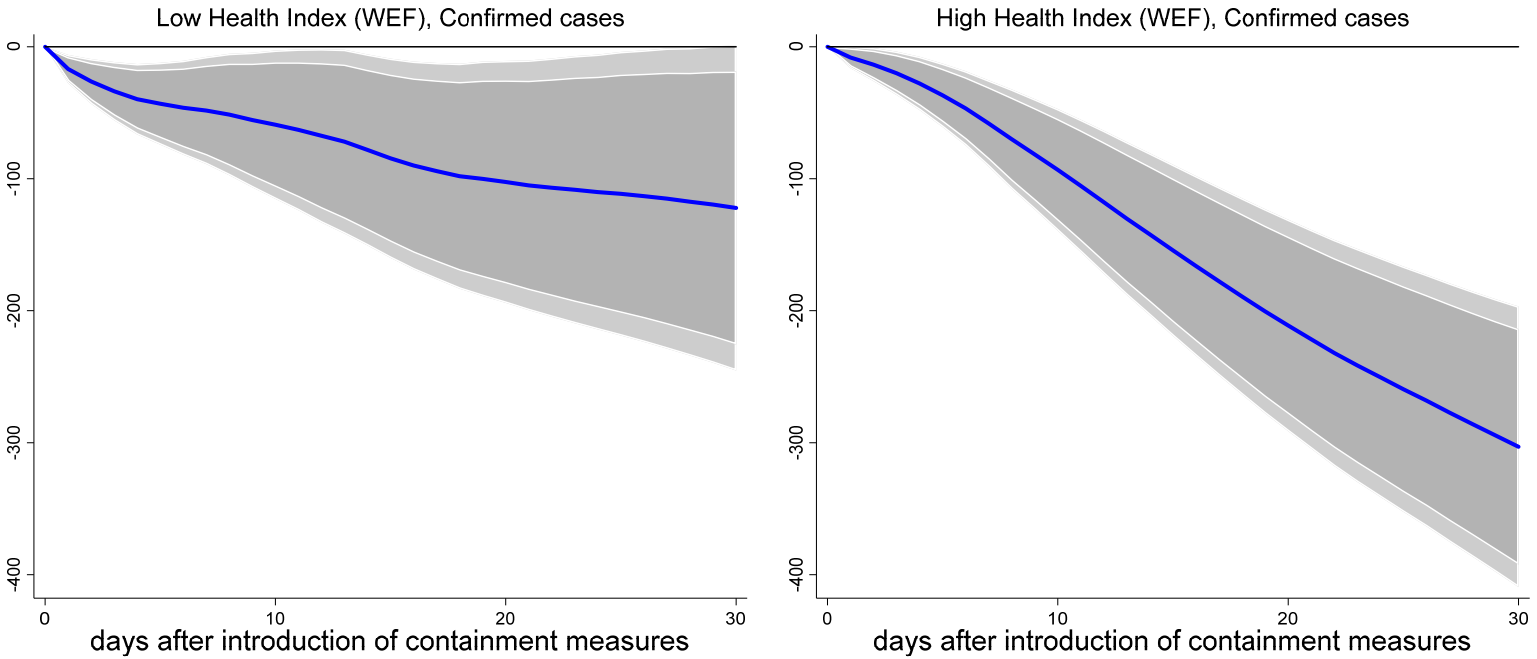

Note: Impulse response functions are estimated using a sample of 129 countries using daily data from the start of the outbreak. The analysis is restricted to countries with a significant outbreak that has lasted at least 30 days. The graph shows the response and confidence bands at 90 and 95 percent. The horizontal axis shows the response x days after the containment measures. Estimates based on $\Delta d_{i,t+h} = u_i + u_t + \theta_h^L F(z_{i,t}) c_{i,t} + \theta_h^H (1 - F(z_{i,t})) c_{i,t} + X'_{i,t}\Gamma_h + \sum_{\ell=1}^{\mathcal{L}} F(z_{i,t})\, \psi_{h,\ell} \Delta d_{i,t-\ell} + \sum_{\ell=1}^{\mathcal{L}} (1 - F(z_{i,t})) \psi_{h,\ell} \Delta d_{i,t-\ell} + \varepsilon_{i,t+h}$ with $F(z_{it}) = \frac{exp^{-\gamma z_{it}}}{(1-exp^{-\gamma z_{it}})}, \gamma > 0$ where $\Delta d_{i,t+h} = d_{i,t+h} - d_{i,t+h-1}$ and $d_{i,t}$ is the logarithm of the number of COVID-19 cases in country i observed at date t and z is the country-specific characteristics normalized to have zero mean and a unit variance. The model is estimated at each horizon $h = 0, 1, \ldots H$, with a lag structure $\ell = 1, 2 \ldots \mathcal{L}$; $c_{i,t}$ is the index capturing the level of containment and mitigation measures; X is a matrix of time varying control variables and country specific linear, quadratic and cubic time trend. Results are based on June 15 data. The figure displays log-difference changes whereas the text translates these into percent changes.